IOP Publishing New J. Phys. 17 (2015) 103035 doi:10.1088/1367-2630/17/10/103035

New Journal of Physics
The open access journal at the forefront of physics

Deutsche Physikalische Gesellschaft DPG
IOP Institute of Physics

Published in partnership with: Deutsche Physikalische Gesellschaft and the Institute of Physics

OPEN ACCESS

RECEIVED
26 June 2015

REVISED
1 September 2015

ACCEPTED FOR PUBLICATION
9 September 2015

PUBLISHED
16 October 2015

Content from this work may be used under the terms of the Creative Commons Attribution 3.0 licence.

Any further distribution of this work must maintain attribution to the author(s) and the title of the work, journal citation and DOI.

PAPER

Frequency-dependent selection at rough expanding fronts

Jan-Timm Kuhr and Holger Stark

Institut für Theoretische Physik, Technische Universität Berlin, Hardenbergstrasse 36, 10623 Berlin, Germany

E-mail: jan-timm.kuhr@tu-berlin.de

Keywords: range expansion, surface growth, evolutionary game theory, non-equilibrium phase transition, kinetic roughening, evolution

Abstract

Microbial colonies are experimental model systems for studying the colonization of new territory by biological species through range expansion. We study a generalization of the two-species Eden model, which incorporates local frequency-dependent selection, in order to analyze how social interactions between two species influence surface roughness of growing microbial colonies. The model includes several classical scenarios from game theory. We then concentrate on an expanding public goods game, where either cooperators or defectors take over the front depending on the system parameters. We analyze in detail the critical behavior of the nonequilibrium phase transition between global cooperation and defection and thereby identify a new universality class of phase transitions dealing with absorbing states. At the transition, the number of boundaries separating sectors decays with a novel power law in time and their superdiffusive motion crosses over from Eden scaling to a nearly ballistic regime. In parallel, the width of the front initially obeys Eden roughening and, at later times, passes over to selective roughening.

1. Introduction

Living species are usually confined to their territory, a spatial region defined by geographical borders, climate, or other environmental constraints. Uninhabited regions are colonized through range expansion, where individuals reproduce and disperse at the front of their territory [1]. This process is seen in biological invasions [2], as a result of shifting climate zones [3–5], during colonizations in our own species' history [6–8], tumor growth [1, 9, 10], and biofilm growth [11–13]. Evidently, expansions occur on very different spatial (micrometers to 10^7 m) and temporal (hours to millennia) scales.

In this article we aim to characterize range expansion under the influence of short-range 'social interactions' of individuals at the front. Such interactions are present if success in reproduction depends on the presence of nearby individuals of the own and/or other species. Here, we set up a model for the expanding front based on evolutionary game theory [14–16] and investigate its roughening dynamics for two interacting species. Besides exploring an interesting non-equilibrium growth process, we hope to contribute to interpreting experiments on range expansion in multi-species colonies of simple organisms.

In experiments, microbial growth is excellently suited to study range expansion and other processes in population dynamics and evolution such as spatial spread of infections and adaptation to an environment (see for example [17]). Microbes reproduce fast, their environment and genotype can be controlled, and experimental conditions are easily reproducible. Grown in a Petri dish, the spatial patterns of single-species microbial colonies have long been a rich field of study [18–23]. The observed patterns crucially depend on motility, availability of nutrients, growth medium, and adhesion between cells, to name but a few. However, even under conditions of negligible motility and abundant nutrients a colony's front is rough and has interesting statistical properties [24–26].

Multi-species colonies are composed of more than one species and show additional intriguing features, even if the species are identical except for a marker [27]. During reproduction they keep their marker but compete with other species for space at the front. Thereby, *sectors of single species* form, which are separated by *boundaries*.

© 2015 IOP Publishing Ltd and Deutsche Physikalische Gesellschaft

Their statistical and dynamic properties are determined by the evolving roughness of the expanding front [28, 29].

Usually, when two or more species of microbes live in a common environment, they influence each other during reproduction. In particular, reproductive success of any species, also called its fitness, depends on the population sizes of all the species. This constitutes 'social interactions' between the species commonly referred to as *frequency-dependent selection*. Research in the field has initiated a wealth of fascinating experiments [10, 30–36] either in well-mixed liquid culture without any spatial order [32, 37] or in the Petri dish, where the populations are spatially structured [38, 39]. Many of the experimental observations can be discussed within the framework of evolutionary game theory [14–16]. For example, light has been shed on a long-standing theoretical question in evolution [14, 15, 40–42]: Why do individuals cooperate if non-cooperators can exploit them? Literature emphasizes the importance of a population to be structured in groups [15, 43–47], for example, by spatial distance. While within a single group cooperators are always inferior to non-cooperating defectors, if the latter interact only with their neighborhood, distant large groups of cooperators will ultimately outcompete defectors. Some models also stress the central role of demographic fluctuations and of populations growing in size [48, 49]. Both, experiments and theory, explain the advantage of cooperators during colony growth by their ability to locally advance faster [39, 50, 51], vividly termed 'survival of the fastest' [39].

Cooperation between between nearby cells is often mediated by some biochemical compound (a *public good*) which the microbes release into the extracellular environment. This compound then promotes reproduction of neighboring cells. In general, a released substance may act beneficial or detrimental to other individuals, also depending on their species, and implies some cost to the producer. Examples include secretion of digestive invertase to break down sucrose [37, 52–54], siderophores to scavenge iron from the environment [32, 55, 56], polymers which support biofilms [43, 57, 58], release of toxins [59, 60] (sometimes through lysis [61, 62]), surfactants which facilitate swarming [63], and the exchange of amino acids [38].

This plethora of biochemical compounds, released by cells and affecting nearby cells, implies a wealth of specific features, which certainly are not covered by a single model. However, since the released biomolecules usually mediate short-range interactions between individuals, properties on large scales should be independent of microscopic details. Hence, we formulate a simple model which captures the essence of an interaction while ignoring complicated details. The classical Eden model [64, 65], a simple growth process on a lattice, has been used successfully to mimic growing cell colonies. It generates a cluster (the colony), the surface of which exhibits scaling properties also found for expanding fronts of microbial colonies [66, 67]. Extended to two identically growing but still distinguishable species, it generates sectors occupied by a single species only [29, 68]. Indeed, this behavior is found for two-species microbial colonies [27]. Moreover, boundaries between sectors move superdiffusively as in the experiments.

In this article we explore a generalization of the two-species Eden model, which incorporates local frequency-dependent selection. We thereby aim to analyze how social interactions influence surface roughness of growing microbial colonies. We set up an expanding public goods game, where either cooperators or defectors take over the front depending on the system parameters [14–16]. Right at the transition the front displays critical behavior, which we analyze in detail. In particular, we establish that our model belongs to a new universality class of phase transitions dealing with absorbing states. At the transition, the number of boundaries separating sectors decays with a novel power law in time and their superdiffusive motion crosses over from Eden scaling to a nearly ballistic regime. In parallel, the width of the front initially obeys Eden roughening and, at later times, passes over to what we call selective roughening.

The remainder of this article is organized as follows. To analyze multi-species microbial colony growth, we introduce the Eden model with frequency-dependent selection in section 2 and analyze its phenomenology in section 3. We then concentrate on the expanding public goods game with its social dilemma in section 4 and analyze the critical behavior at the transition between long-term cooperation and long-term defection by applying statistical analysis. Finally, we discuss and summarize our findings in section 5.

2. Eden model with frequency-dependent selection

In this work we employ a lattice model (see figure 1) to analyze range expansion at rough fronts under the influence of frequency-dependent selection. We set up a cellular automaton on a two-dimensional hexagonal[1] lattice of transverse extension L and an infinite longitudinal extension. Periodic boundary conditions are applied in the transverse direction. The state $\{s\}$ of the system at time t is specified by the state variables $s_{i,j}$ of lattice sites (i, j). Consider a system with two species (extension to more species is straightforward). For any time t, any site

[1] On a square lattice it is impossible to enclose a cluster A within a cluster B, which only contains nearest neighbor sites of cluster A. On a hexagonal lattice this is possible.

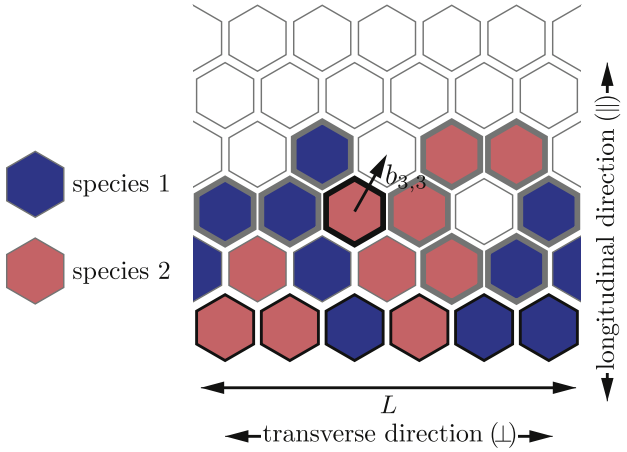

Figure 1. Two-species Eden model with frequency-dependent selection on a hexagonal lattice. The bacterial colony grows from the bottom line (lattice sites with narrow black edge) of length L, where individuals of species 1 (blue) and species 2 (red) occupy the lattice sites. The colony expands into the empty, infinitely-extended half-space. Individuals capable of reproduction (indicated by bold edges), have at least one empty lattice site as a nearest neighbor. In a reproduction event, one of these empty neighboring sites (i, j) is chosen with equal probability and the reproducing individual changes the corresponding state $s_{i,j}$ to its own state 1 or 2. Each individual has its own reproduction rate $b_{i,j}$ given in equation (1). For example, the reproduction rate of the individual at site (3, 3) (bold black edge) is $b_{3,3} = b_2^0 + 3\mathcal{T} + 2\mathcal{P}$. Along the transverse direction periodic boundary conditions apply.

(i, j) is either empty ($s_{i,j} = 0$) or occupied by an individual of either species 1 ($s_{i,j} = 1$) or 2 ($s_{i,j} = 2$). All individuals which have at least one free nearest neighbor site can reproduce. To perform a reproduction step, we choose one of these fecund individuals with a probability proportional to its reproduction rate (see below) and a new individual of the same species is placed with equal probability on one of the free neighboring sites.

In contrast to the Eden model [64] and some of its two-species generalizations [29, 69], reproduction rates in our model depend on the states of the nearest-neighbor sites. Let n_1 and n_2 denote the number of nearest neighbors of species 1 and 2, respectively, then the reproduction rate of an individual at lattice site (i, j) is

$$b_{i,j} = \begin{cases} 0 & \text{if } s_{i,j} \text{ has no free neighbors,} \\ b_1^0 + n_1\mathcal{R} + n_2\mathcal{S} & \text{if } s_{i,j} = 1, \\ b_2^0 + n_1\mathcal{T} + n_2\mathcal{P} & \text{if } s_{i,j} = 2. \end{cases} \tag{1}$$

Here, b_1^0 and b_2^0 are the respective contributions to the reproduction rates of species 1 and 2, which are independent of the states of their nearest neighbors. Frequency-dependent selection is introduced through the parameters $\mathcal{R}$, $\mathcal{S}$, $\mathcal{T}$, and $\mathcal{P}$.

With the reproduction rates $b_{i,j}$ we implement a random sequential update of the system using a simplified version of the Gillespie algorithm [70]. The overall reproduction rate of the population is $b_{\text{tot}} := \sum_{i,j} b_{i,j}$ and an individual at site (i, j) is selected to reproduce with probability $b_{i,j}/b_{\text{tot}}$. We then choose one of the empty nearest-neighbor sites of the reproducing individual at random and place there a new individual of the same species. This implies that there are no mutations. Since the mean time until the next reproduction event is b_{tot}^{-1}, we update time by $t \to t + b_{tot}^{-1}$ after each reproduction event. We assume that individuals do not die and that they are immobile. Therefore, any site with $s_{i,j} \neq 0$ remains in its specific state indefinitely. As initial condition we occupy all sites of an initial line randomly, but in equal parts, with species 1 and 2, if not stated otherwise.

The formulated model generalizes version C of the Eden model, introduced by Jullien and Botet [71], to a two-species system. We already applied a similar model to range expansion without frequency-dependent selection but included the possibility of mutations [69]. If $\mathcal{R}$, $\mathcal{S}$, $\mathcal{T}$, and $\mathcal{P}$ are zero, our model reduces to that of Saito and Müller-Krumbhaar [29], however they used a square lattice. Since diffusion is not included in the model, configurations and patterns behind the front are frozen. This corresponds to observations in microbial experiments on range expansion [27, 62]. Our model does not include adhesion between cells, which contributes to surface tension and can thus smooth the surface of a bacterial colony [23]. It also ignores the vertical extension of bacterial colonies since the horizontal extension is usually larger by several orders of magnitude.

In game theory the parameters $\mathcal{R}$, $\mathcal{S}$, $\mathcal{T}$, and $\mathcal{P}$ from equation (1) define the payoff matrix of a two-strategy game [14–16]. Different scenarios, some well known in game theory, are implemented if we set these parameters accordingly.

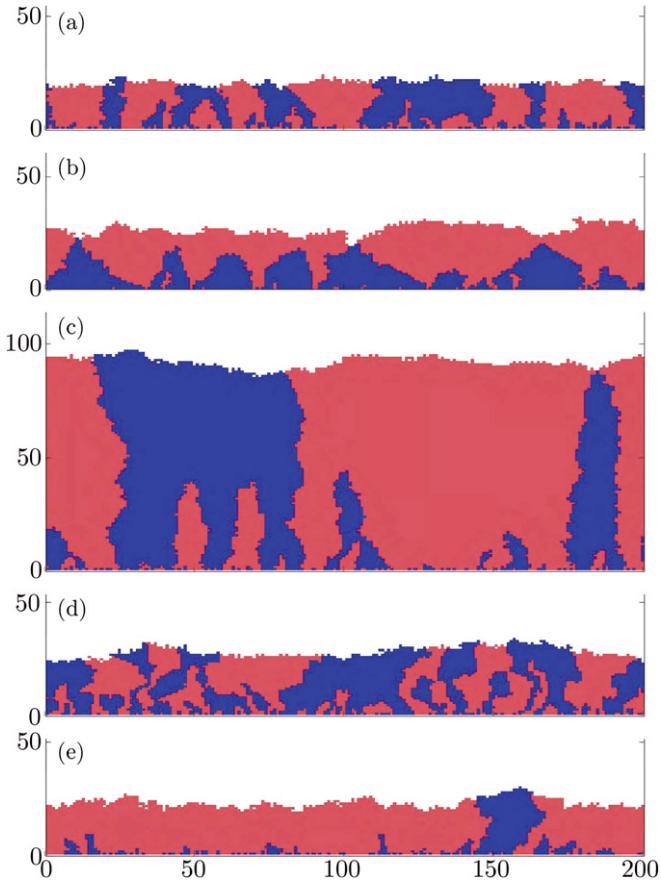

Figure 2. Growth patterns of our model for different parameters, which correspond to typical settings. Time is always $t = 15$ and lattice size is $L = 200$. Cooperators are depicted in blue and defectors in red. If not stated otherwise $b_2^0 = b_2^0 = 1$, $\mathcal{R} = \mathcal{P} = \mathcal{S} = \mathcal{T} = 0$, and the initial ratio of both species is 1:1. (a) Neutral growth, (b) selective advantage for species 2 ($b_2^0 = 1.5$), which occupies 10% of initial sites, (c) coordination game ($\mathcal{R} = \mathcal{P} = 1$), (d) snowdrift game ($\mathcal{S} = \mathcal{T} = 1$), and (e) public goods game ($\mathcal{R} = 0.1$, $\mathcal{T} = 1.1$).

3. Phenomenology

We now describe some generic examples of our model for growing microbial colonies (see figure 2), which emerge for typical parameter settings, and discuss their characteristic features. We then concentrate on so-called social dilemmas, where one species (defectors) exploits the other one (cooperators). Due to the spatial extent of our system, cooperators are able to outcompete defectors in a defined parameter region. This is in contrast to a single group, where all members interact with each other and, therefore, cooperators are always inferior to defectors.

In the simplest case selection is frequency-independent, $\mathcal{R} = \mathcal{S} = \mathcal{T} = \mathcal{P} = 0$, and both species reproduce with the same rate, $b_0^1 = b_0^2$ (see figure 2(a)). For this 'neutral' setting we observe roughening of the front typical for the Eden model [64, 65]. Simultaneously, sectors composed of a single species merge and thereby coarsen [29, 68]. This inherent process happens according to the following scenario. If the tips of two advancing boundary lines meet, they annihilate and the enclosed sector loses contact to the front. Consequently, the number of boundaries and sectors can only decrease. Sectors repeatedly coarsen as they merge in these events. When all boundaries have vanished, the front 'has fixed' to a single species, which keeps on expanding. In finite systems, $L < \infty$, fixation to a single species always occurs since in our stochastic model there is always a finite rate at which boundaries annihilate. Hence, two absorbing states exist. Eventually, the expanding front will fix either to species 1 or species 2.

In figure 2(b), species 2 has a larger reproduction rate, $b_0^2 > b_0^1$, and therefore a constant selective advantage. As the front expands faster at locations where it is composed of species 2, the roughness of the front increases. Indentations of the front usually are caused by sectors of species 1, whereas species 2 creates bulges. Furthermore, boundaries are biased such that sectors of species 2 widen while sectors of species 1 shrink laterally. Hence, sectors of species 2 merge and coarsen quickly. Eventually, the expanding front will fix to species 2, which has almost happened in figure 2(b).

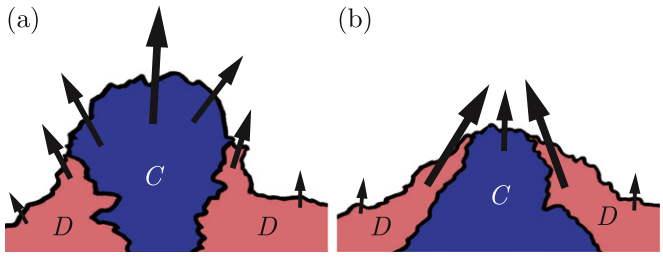

Figure 3. Schematics of possible scenarios in an expanding public goods game. Depending on the parameters $\mathcal{R}$, $\mathcal{S}$, $\mathcal{T}$, and $\mathcal{P}$ of equation (1), cooperators (C, blue) and defectors (D, red) advance with different speeds, as indicated by arrows. (a) Cooperators outrun the trailing defectors. From an advanced position along the front cooperators can then expand laterally and take over the front. (b) A thin layer of defectors keeps up with the cooperators' sector and, eventually, completely covers the cooperators.

If the reproduction rates depend on the state of nearest neighbors (frequency-dependent selection), new patterns arise. In this article we are mainly interested in frequency-dependent selection and therefore set $b_1^0 = b_2^0 = 1$ from here on. We now discuss some interesting cases, see figures 2(c) and (d), which correspond to well-known settings in game theory [14–16].

In coordination games ($\mathcal{R} > \mathcal{T}$ and $\mathcal{P} > \mathcal{S}$), see figure 2(c), the front expands slower near boundaries than in the centers of sectors. Therefore, indentations in the front are typically found where boundaries currently are or recently have been. After sectors have coarsened for some time, most individuals are located inside sectors. Therefore, most of them only have neighbors of their own kind, which raises the average reproduction rate and the overall front advances faster.

In snowdrift games ($\mathcal{R} < \mathcal{T}$ and $\mathcal{P} < \mathcal{S}$), see figure 2(d), the front expands faster near boundaries. They annihilate less frequently as compared to figure 2(c) since narrow sectors grow faster. Boundaries are also strongly twisted and associated with bulges of the front.

In this article we are mostly interested in social dilemmas where one species (called cooperators) raises the reproduction rate of all neighbors regardless of their species. The increased reproduction rate is called a *public good* in game theory, since it is of benefit to all nearby individuals, but it also costs resources. In contrast, the other species (called defectors) takes advantage of the public good for its own reproduction, but does not contribute to the reproduction of its neighbors in the same way. Defectors save resources for their own reproduction and therefore have an advantage. In this scenario defectors do not at all contribute to reproduction of their neighbors and, therefore, we set $\mathcal{S} = \mathcal{P} = 0$ and just vary $\mathcal{R}$ and $\mathcal{T}$. According to equation (1), these two parameters increase the respective reproduction rates of cooperators and defectors if they have cooperating neighbors. In figure 2(e) we present a setting, where species 2 (defectors) rapidly takes over large parts of the front. Defectors benefit from the initially large number of boundaries, where they take advantage of nearby cooperators, and conquer most of the front. Only cooperators, living in sufficiently large sectors, can keep up with the front during this early period and may then take over the front, depending on the parameter values.

In a situation like this, it is not *a priori* clear if the front eventually fixes either to cooperators or to defectors. Depending on the values of $\mathcal{R}$ and $\mathcal{T}$, cooperators can either outrun defectors and, from their advanced position at the front, overgrow their competitors laterally, see figure 3(a). Or, defectors cover cooperators with a thin layer and thereby take over the front, see figure 3(b). Close to the transition between both scenarios, the front displays increasing roughness since both species are able to take over while their fronts grow with different speeds. To characterize this transition quantitatively, we performed extensive simulations and applied methods from surface roughening [65, 72–74] and the theory of phase transitions dealing with absorbing states [74, 75].

4. Expanding public goods game: critical behavior

In this section we quantitatively analyze the transition between long-term cooperation and long-term defection for an expanding public goods game. As the transition is approached, several observables show critical scaling [74, 75]. Following our earlier work [69], we perform finite-size scaling to localize the transition. Furthermore, we determine critical exponents and thereby establish a new universality class for the transition between the two adsorbing states. In the vicinity of the transition we also study the dynamics of the sector boundaries including the decline of their mean number during coarsening and their superdiffusive motion as well as the roughening of the expanding front.

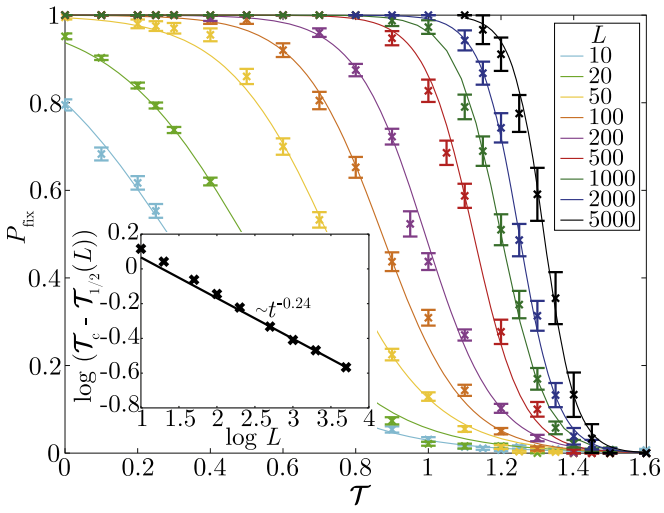

Figure 4. Probability P_{fix} of the front to fix to cooperators plotted versus $\mathcal{T}$ for several system sizes L at $\mathcal{R} = 0.1$. Error bars give the standard error of the mean for each data point. Lines are fits of the data points to the Fermi function, $1/[\exp(c(\mathcal{T} - \mathcal{T}_{1/2})) + 1]$, where $\mathcal{T}_{1/2}$ and c are fit parameters. Inset: The transition point $\mathcal{T}_{1/2}(L)$ relative to the fitted critical value $\mathcal{T}_c \approx 1.58$ (black crosses) follows a power law in $L \to \infty$: $\mathcal{T}_c - \mathcal{T}_{1/2}(L) = (A/L)^{1/4.2}$ (black line).

4.1. Finite-size scaling and phase diagram

As boundaries merge, sectors coarsen and the system progresses towards one of the two absorbing states. At finite system sizes L this is a stochastic process and both adsorbing states are reached with a certain probability. However, in the thermodynamic limit, $L \to \infty$, the magnitude of fluctuations relative to the mean value goes to zero and one of the absorbing states is reached with certainty. We now use the method of finite-size scaling to determine the transition point between both states [75].

In figure 4 we present the probability P_{fix} that the front fixes to cooperators and plot it versus $\mathcal{T}$ for several lattice sizes L at $\mathcal{R} = 0.1$. We distinguish two regimes: one where cooperators dominate ($P_{\text{fix}}(\mathcal{T}, L) > \frac{1}{2}$) and one where defectors take over. We locate the transition point at $\mathcal{T}_{1/2}(L)$ by $P_{\text{fix}}(\mathcal{T}_{1/2}(L), L) = \frac{1}{2}$. $P_{\text{fix}}(\mathcal{T}, L)$ is a monotonically decreasing function in $\mathcal{T}$ of sigmoidal shape. We use a Fermi function to fit it and extract the transition point, see figure 4. Other sigmoid functions (e.g. Hill equation, hyperbolic tangent) gave qualitatively identical results, but with reduced fit quality and hence lower accuracy. As $L \to \infty$, P_{fix} converges to a step function, since in infinite systems the absorbing states are reached with certainty. The step is positioned at $\mathcal{T}_c := \lim_{L\to\infty} \mathcal{T}_{1/2}(L)$. From the theory of critical scaling applied to absorbing states, we expect that close to the critical point $\mathcal{T}_c$ the states of the lattice sites are correlated on the transverse distance $\xi_\perp$. Approaching $\mathcal{T}_c$, $\xi_\perp$ diverges as $|\Delta|^{-\nu_\perp}$, where $\Delta := \mathcal{T}_c - \mathcal{T}$ is the distance to the critical point and $\nu_\perp$ is a *critical exponent*. For finite systems, an absorbing state is reached if

$$L \approx \xi_\perp \sim |\Delta|^{-\nu_\perp}. \tag{2}$$

The transition occurs at $\mathcal{T}_{1/2}(L)$ and rearranging equation (2), we obtain

$$\mathcal{T}_{1/2}(L) \approx \mathcal{T}_c - (A/L)^{1/\nu_\perp}. \tag{3}$$

The characteristic length A is related to the microscopic length scale, which here is the lattice constant, and details of our model. It is not important to the following analysis. The inset of figure 4 shows the best fit of our data to equation (3), which yields the critical exponent $\nu_\perp \approx 4.2$ and the critical point $\mathcal{T}_c \approx 1.58$ at $\mathcal{R} = 0.1$. Note that the parameter c^{-1} of our Fermi fit function gives the width of the transition region in $\mathcal{T}$. Within this region transverse fluctuations in the boundaries are typically larger than or comparable to L, from which $c \sim L^{1/\nu_\perp}$ follows. This is indeed observed and corroborates our scaling analysis (data not shown).

The above procedure can be repeated for different values of $\mathcal{R}$ to map out the phase diagram (see figure 5). One realizes that the benefit of cooperators from their own species, $\mathcal{R}$, has a much more pronounced influence on the final state than the defectors' benefit from cooperating neighbors, $\mathcal{T}$. This makes sense, since at large times $t \gg 1$ the front contains large single-species sectors. Hence, the number of sector boundaries N_b, where defectors can benefit from cooperators, is small: $N_b \ll L$. Therefore, almost all cooperators have cooperating neighbors, while only a few defectors have this advantage. This is an example of 'preferential assortment', where the benefit of cooperation is almost entirely available to other cooperators [15, 32, 33, 45–47, 76, 77]. So, for a wide range of parameter combinations cooperators can indeed outcompete defectors. However, for large

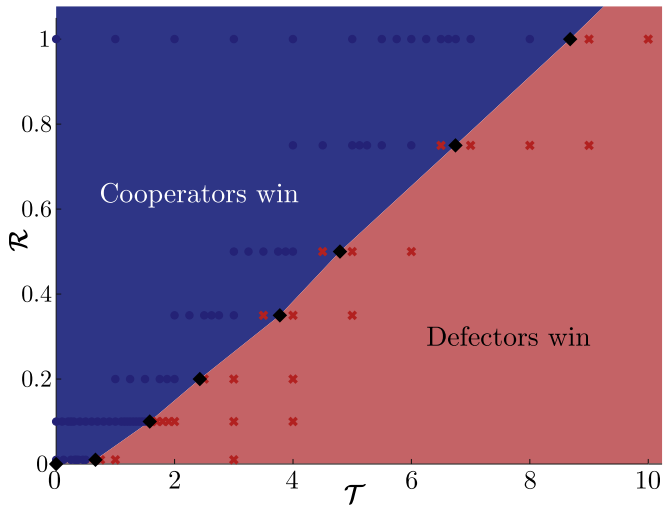

Figure 5. Phase diagram of the two-species public goods game with range expansion. Parameter regimes, where the expanding front fixes either to cooperators or defectors in large systems with $L \to \infty$, are indicated by blue and red shade, respectively. Red crosses are from simulations with system size $L = 1000$, where defectors always outcompeted cooperators ($P_{\text{fix}} = 0$) while blue dots identify events where cooperators survived ($P_{\text{fix}} > 0$). The black diamonds indicate critical points $\mathcal{T}_c$ for $L \to \infty$ determined from finite-size scaling (see equation (3) and figure 4). Note that in finite systems defectors have an advantage in a larger parameter region.

enough $\mathcal{T}$ the dynamics at the boundaries still determines the final state of the front and defectors outcompete cooperators.

4.2. Critical exponents of the phase transition

In the previous section 4.1 we already encountered the critical exponent $\nu_\perp$. We now continue to determine further critical exponents of the phase transition. They are universal, which means independent of microscopic details. The exponents only depend on the dimension of the system, the number of components of the order parameter, and symmetries of the model [74, 75]. Our system has properties similar to 'compact directed percolation' (CDP) [78]. This is a stochastic process with a flat front, which also has two distinct absorbing states. Using this similarity, we proceed by determining critical exponents, which are known for CDP [75], and compare both models.

At the critical transition, $\mathcal{T} = \mathcal{T}_c$, none of the two species has an advantage. Heterogeneous fronts, composed of more than one sector, exist for long times before the front fixes to one of the absorbing single-species states. This can be quantified by the mean time to fixation, t_{fix}, presented in figure 6. The data show that the fixation time has a maximum, the position and value of which grow with system size.

Along the longitudinal direction, in which the front propagates, states are correlated on the longitudinal distance $\xi_\parallel$. As before, we expect it to scale like $|\Delta|^{-\nu_\parallel}$ close to the transition. Since the front propagates with a mean velocity, $\xi_\parallel$ is proportional to a correlation time. Close to $\mathcal{T}_c$ this time becomes very long, which is known as critical slowing down. Substituting equation (2) into $\xi_\parallel \sim |\Delta|^{-\nu_\parallel}$, we find the scaling relation

$$\xi_\parallel \sim L^{\nu_\parallel/\nu_\perp}. \tag{4}$$

We expect the mean fixation time to be proportional to the correlation time $\sim\xi_\parallel$. Therefore, in the inset of figure 6 we plot t_{fix} rescaled by $L^{\nu_\parallel/\nu_\perp}$ versus Δ rescaled by $L^{-1/\nu_\perp}$. All curves of the main plot collapse on a single master curve for $\mathcal{T}_c = 1.59 \pm 0.03$, and critical exponents $\nu_\perp = 4.2 \pm 0.1$ and $\nu_\parallel = 3.5 \pm 0.1$. The values of $\mathcal{T}_c$ and $\nu_\perp$ are in good agreement with our fit to equation (3). So, fixation of the front is determined by the characteristic time

$$\tau_{\text{fix}} \sim \xi_\parallel \sim L^{0.83\pm0.05}. \tag{5}$$

Two more critical exponents right at the transition are related to the survival probability of one species or state, which initially occupies a single site while all the other sites are occupied by the other state. We choose a single cooperator site in a line of defectors and determine the probability $P_C(t)$ that after time t there are still cooperators at the front and also calculate the average number of cooperator sites at the front, $N_C(t)$. In figure 7 we plot both quantities versus time for different defector benefit $\mathcal{T}$. At the transition situated between $\mathcal{T} = 1.55$ and 1.6, we find that both P_C and N_C (see inset) decay with power laws in time: $P_C(t) \sim t^{-\beta'/\nu_\parallel}$ and $N_C(t) \sim t^{-\Theta}$. The respective best fits yield $\beta'/\nu_\parallel = 2.2 \pm 0.1$ and $\Theta = 1.3 \pm 0.1$. Using our result for $\nu_\parallel$, we find $\beta' = 7.7 \pm 0.6$.

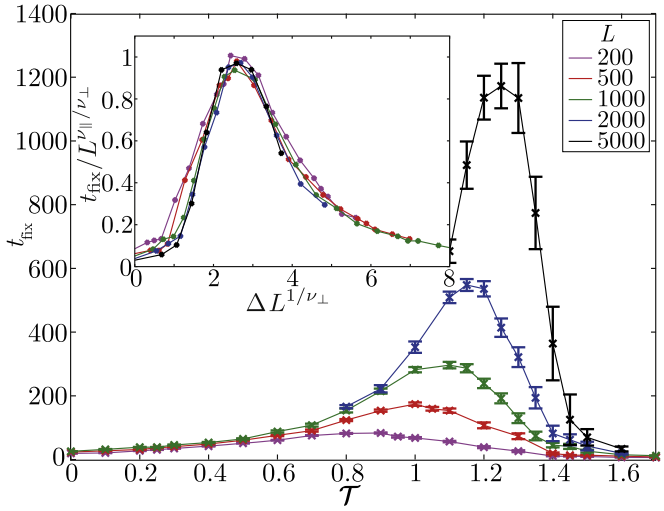

Figure 6. Mean time to fixation $t_{\rm fix}$ as a function of defector benefit $\mathcal{T}$ for various system sizes L at $\mathcal{R} = 0.1$. The inset depicts the rescaled fixation time, where $\Delta = \mathcal{T}_c - \mathcal{T}$ All data collapse on a single master curve for critical exponents $\nu_\parallel = 3.5 \pm 0.1$ and $\nu_\perp = 4.2 \pm 0.1$ and critical point $\mathcal{T}_c = 1.59 \pm 0.03$. Accordingly, $t_{\rm fix}$ grows with L and the position of its maximum approaches $\mathcal{T}_c$ for $L \to \infty$.

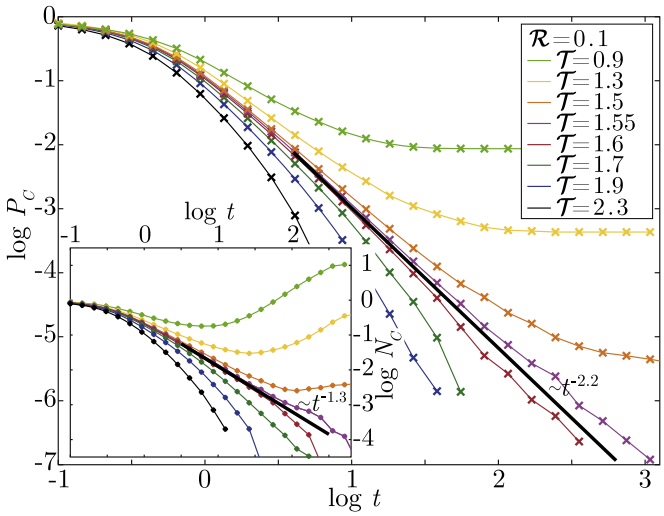

Figure 7. Survival probability P_C of cooperators starting from a single site plotted versus time for several values of $\mathcal{T}$ Other parameters are $L = 1000$ and $\mathcal{R} = 0.1$. For $T > \mathcal{T}_c$, P_C decreases exponentially, while for $T < \mathcal{T}_c$ the front fixes to cooperators with a non-zero probability. At the transition point $\mathcal{T}_c$, the survival probability decays in time with a power law with exponent $\beta'/\nu_\parallel = 2.2 \pm 0.1$. Inset: The number of cooperator sites at the front, N_C, decays exponentially in time for $T > \mathcal{T}_c$ and is non-monotonic for $T < \mathcal{T}_c$. At the transition N_C decreases with a power law with critical exponent $\Theta = 1.3 \pm 0.1$.

In general, in phase transitions to absorbing states the critical exponent β governs the stationary density of 'active sites', when approaching the transition [75]. In our case, the 'active' sites can either be cooperators or defectors. Since the stationary state is either an all cooperator or an all defector front, the density $\sim|\mathcal{T}_c - \mathcal{T}|^\beta$ jumps from 0 to 1 and hence β is 0. Our results for all the critical exponents are summarized in table 1 together with the exponents of some related universality classes. We also give the critical exponents for the neutral transition point $\mathcal{R} = \mathcal{T} = 0$, which were obtained by similar means (data not shown). For this case the scaling of the time to fixation $\tau_{\rm fix}$, and therefore the ratio $\nu_\parallel/\nu_\perp = 3/2$, can be determined from the annihilation dynamics of the boundaries (see section 4.3).

The neutral system $\mathcal{R} = \mathcal{T} = 0$ is symmetric in the behavior of cooperators and defectors and therefore closely related to CDP, where active and inactive sites are interchangeable. It may therefore be called a 'rough CDP'. The roughness of the front evolves through kinetic roughening and is identical to the one-species Eden model. When the transition occurs at non-zero $\mathcal{R}$ and $\mathcal{T}$, the symmetry between the two species is missing. Indeed, cooperator and defector sectors expand differently, which we regard as the reason for the different

Table 1. Critical exponents for the phase transition to the absorbing states (either long-term global defection or long-term global cooperation) for the expanding public goods game with frequency dependent selection. The neutral case $\mathcal{R} = \mathcal{T} = 0$, which has different scaling, is also included. For comparison we also give the exponents for CDP [75, 78] and for an earlier work on rough range expansion [69].

	$\nu_\perp$	$\nu_\parallel$	β	β'	Θ
$\mathcal{R}, \mathcal{T} > 0$	4.2 ± 0.1	3.5 ± 0.1	0	7.7 ± 0.6	1.3 ± 0.1
$\mathcal{R} = \mathcal{T} = 0$	0.75 ± 0.05	1.1 ± 0.1	0	0.9 ± 0.2	0.02 ± 0.01
$1d$ CDP	1	2	0	1	0
[69]	1.6 ± 0.1	1.6 ± 0.1	0.50 ± 0.02	0.51 ± 0.07	0.32 ± 0.02

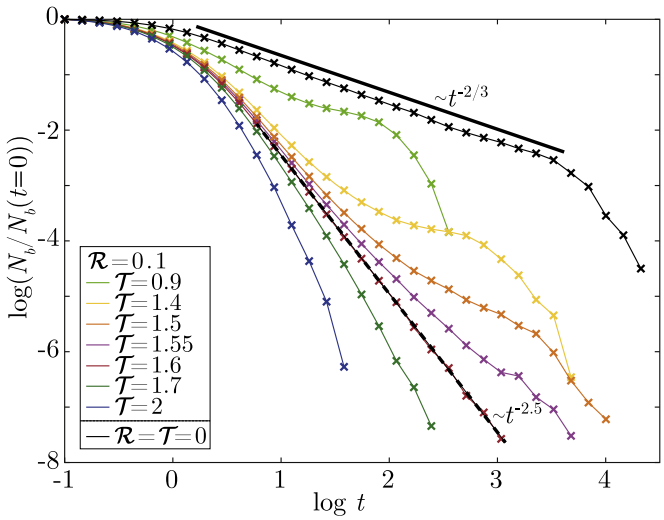

Figure 8. Mean number of sector boundaries N_b plotted as a function of time for several values of $\mathcal{T}$. Other parameters are $L = 1000$ and $\mathcal{R} = 0.1$. Solid black line: $N_b(t) \sim t^{-2/3}$, as predicted in [29] for neutral growth ($\mathcal{T} = \mathcal{R} = 0$). At large times the simulated curve deviates from the power law due to finite system size. Dashed black line: Close to the critical point $\mathcal{T} = \mathcal{T}_c \approx 1.6$, we find a power-law decay $N_b(t) \sim t^{-2.5}$.

critical exponents. We study surface roughening of the expanding fronts in more detail in section 4.4. When approaching the neutral point $\mathcal{R} = \mathcal{T} = 0$ along the phase transition line, we expect to find crossover behavior. Following [79] we determined the crossover exponent ϕ by mapping out the phase transition line close to the neutral point and by fitting with $\mathcal{R}_c \sim \mathcal{T}_c^{\phi}$ (data not shown). We obtained $\phi = 1.6 \pm 0.1$.

The set of critical exponents determines the universality class of a phase transition. To our knowledge no other non-equilibrium transition has been found, which shares the same set of exponents. Hence, the transition between long-term cooperation and long-term defection in our expanding public goods game with frequency dependent selection constitutes a new universality class.

4.3. Dynamics of boundaries

In this section we investigate the dynamics of the boundaries which separates sectors of cooperators and defectors from each other. In rough fronts the local front orientation is tilted against the main growth direction. When the front grows further, this tilt directs the movement of boundaries [27, 29]. Ultimately, when two of them meet, they annihilate. In figure 8 we plot their mean number N_b versus time for several values of the defector benefit $\mathcal{T}$. Right at the transition (dashed black line), N_b shows a power law decay. We now discuss the different regimes in figure 8.

For neutral systems, where frequency-dependent selection is absent ($\mathcal{T} = \mathcal{R} = 0$), any inclination of the front is created by stochastic surface or Eden roughening [65, 72–74]. The surface undulations obey KPZ-scaling [80] and thereby drive the decay of N_b [27, 29]. Boundaries move superdiffusively along the front with a mean-square displacement proportional to $t^{4/3}$ [28]. On average, they annihilate after having traveled the mean distance L/N_b between the boundaries, for which they need the time $\sim (L/N_b)^{3/2}$. Hence, boundaries annihilate with a rate proportional to $N_b^{3/2}$, which implies

$$\dot{N}_b \sim -N_b^{3/2} N_b. \tag{6}$$

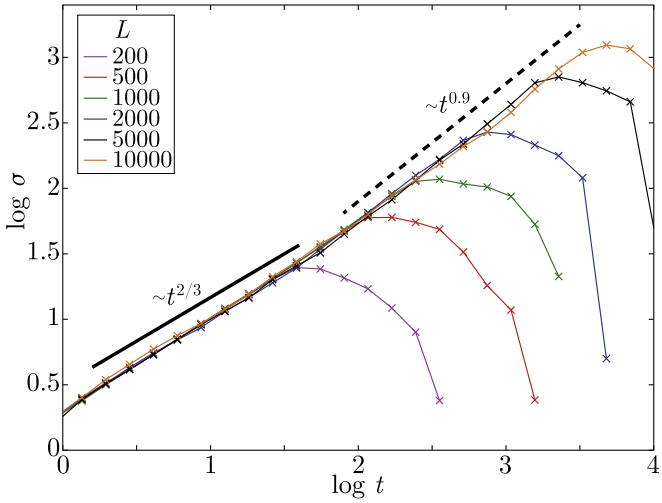

Figure 9. Time evolution of two boundaries with initial distance $L/2$ in a system close to criticality ($\mathcal{T} = 1.6$) and at $\mathcal{R} = 0.1$. Standard deviation σ of the transverse distance plotted versus time t for several system sizes L. The boundaries move superdiffusively. Initially, $\sigma \sim t^{\eta}$ with $\eta = 0.71 \pm 0.05$, and consistent with Eden scaling ($t^{2/3}$, bold black line). At later times a crossover to $\sigma \sim t^{\eta'}$ with $\eta' = 0.9 \pm 0.1$ occurs (dashed black line).

So, the number of boundaries decreases as

$$N_b(t) \sim t^{-2/3}, \tag{7}$$

as already observed by Saito and Müller-Krumbhaar [29]. This power law is excellently reproduced by our simulations in the case of neutral growth, $\mathcal{R} = \mathcal{T} = 0$, as illustrated by the solid black line in figure 8. Equation (7) implies that for $\mathcal{R} = \mathcal{T} = 0$ the time to fixation scales like $L^{3/2}$ since this is the time after which all initially present boundaries with mean number $N_b(t = 0) \sim L$ have annihilated.

For $\mathcal{R} \neq 0$ and $\mathcal{T} \neq 0$, species reproduce with different rates. Hence, the fronts of two neighboring sectors (occupied by different species) advance with different speeds. This influences the tilt of the front orientation, in addition to stochastic roughening in neutral systems, and thereby the movement of the separating boundary. Thus, we do not expect equation (6) to be valid.

Indeed, figure 8 reveals different regimes for the mean number of boundaries N_b. For $\mathcal{T} > \mathcal{T}_c$, N_b decays exponentially in time in line with the exponential decay of the survival probability P_C in figure 7 and similar to the case of selective advantage in [29]. For $\mathcal{T} < \mathcal{T}_c$ boundaries annihilate less frequently. Narrow defector sectors persist in the front dominated by cooperators since almost all individuals in the defector sectors have cooperating neighbors. This results in the upward curvature of the curves in figure 8. However, the defector sectors cannot expand laterally and ultimately loose contact to the front due to random fluctuations, and N_b declines exponentially. At $\mathcal{T}_c$ the number of boundaries decreases with a power law $N_b \sim t^{-\chi}$, where a new exponent $\chi \approx 2.50 \pm 0.05$ appears. This power law implies that the number of boundaries declines from the initial value $N_b(t = 0) \sim L$ to the order of 1 in the coarsening time

$$\tau_{\text{coarse}} \sim L^{1/\chi} \approx L^{0.40 \pm 0.01}. \tag{8}$$

Comparing with equation (5) reveals $1/\chi < \nu_{\parallel}/\nu_{\perp}$. This suggests that for large systems fixing the front to one species takes much longer than coarsening to a few sectors. Hence, the few remaining boundaries move differently compared to early times since they have to annihilate to fix the front to a single species.

To check if this is the case, we employ the initial condition, where the front is composed of only two sectors of size $L/2$ each, separated by two boundaries. We quantify the boundaries' random motion by monitoring the temporal evolution of the standard deviation for the transverse distance $\ell_{\perp}$,

$$\sigma(t) \coloneqq \sqrt{\left\langle \left[\ell_{\perp}(t) - \left\langle \ell_{\perp}(t) \right\rangle \right]^2 \right\rangle}. \tag{9}$$

We subtract the mean distance $\langle \ell_{\perp}(t) \rangle$ to take care of any transient drift, when the front relaxes from its initially flat to the rough shape, and an expected small drift if $\mathcal{T}$ is not exactly $\mathcal{T}_c$.

From figure 9 we see that, for early times, σ grows like a power law, $\sigma \sim t^{\eta}$, with $\eta = 0.71 \pm 0.05$. This is consistent with meandering boundaries induced by Eden roughening, $\sigma \sim t^{2/3}$ [27–29]. We expect such a behavior since the roughness of the front has not fully developed yet. For large systems and later times we find a crossover to $\sigma \sim t^{\eta'}$ with $\eta' = 0.9 \pm 0.1$. This confirms our earlier statement that at late times the few boundaries remaining after coarsening move differently. Indeed, they show an even stronger superdiffusive

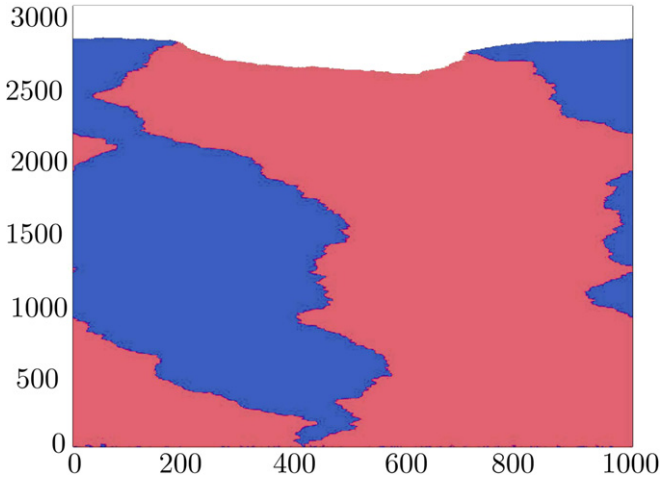

Figure 10. Realization of a system close to criticality ($\mathcal{R} = 0.1$, $\mathcal{T} = 1.55$) before the front fixes to one species. Most cooperator sectors (blue) are rapidly outcompeted by their defecting neighbors (red), but a single cooperator sector survives. Boundaries grow persistently in one direction for long times, superimposed by fluctuations on smaller length scales. This is indicative for the dynamics of sector boundaries close to ballistic scaling, which is expected at late times. The width of the front is dominated by selective roughening: the cooperator sector advances and the defector sector trails behind.

motion than Eden scaling, which is associated with the long-lived and pronounced surface undulations in systems with frequency-dependent selection. To illustrate these findings, a system close to criticality is given in figure 10.

4.4. Surface roughening of the expanding front

We now discuss the surface roughness or undulations of the expanding front and compare our results to the classical Eden model. We measure the roughness of a front by calculating its width w for system size L and at time t:

$$w(L,\, t) := \left(\frac{1}{L} \sum_{i=1}^{L} \Big[h(i,\, t) - \bar{h}(t) \Big]^2 \right)^{1/2}. \tag{10}$$

Here, $h(i,\, t)$ is the longitudinal position of the front at its transverse site i and $\bar{h}(t)$ is the mean position

$$\bar{h}(t) := \frac{1}{L} \sum_{i=1}^{L} h(i,\, t). \tag{11}$$

In the following we will only consider systems where the front has not yet fixed to one species, for parameters close to the phase transition. From equation (5) we know that the time to fixation diverges with system size L. So, in order to extrapolate to $L \to \infty$, we only sample from realizations where the front has not yet fixed to a single species. Figure 11 plots the width $w(L,\, t)$ close to the critical point at $\mathcal{T} = \mathcal{T}_c \approx 1.6$. Initially, the roughness of the front grows like in the original Eden model [64]: $w \sim t^{\gamma}$, where the growth exponent $\gamma = 1/3$ belongs to the KPZ-universality class [65]. At intermediate times a new regime sets in, where $w \sim t^{\gamma'}$ increases with enhanced growth exponent $\gamma' \approx 1.3 \pm 0.1$. This marks the transition from Eden roughening to 'selective roughening'. Here, the typical shape of the front is determined by advancing cooperator sectors and trailing defector sectors (see figure 10). On length scales smaller than the typical extension of a sector one still observes Eden-like roughening. On larger length scales undulations of the front are clearly due to sectors occupied by different species. The resulting large undulations ultimately drive the accelerated increase of the front's width w. The crossover to this regime happens at time $\tau_\times$, which increases with system size L as figure 11 shows. This makes sense since we expect selective roughening to dominate over Eden roughening when the lateral extension of sectors is comparable to L, i.e., $\tau_\times \sim \tau_{\text{coarse}} \sim L^{1/\chi}$. Due to Eden roughening the width at the crossover is $w_\times \sim \tau_\times^{\gamma} \sim L^{\gamma/\chi} \approx L^{0.13}$. Indeed, rescaling width and time with $w_\times$ and $\tau_\times$, respectively, collapses all data in figure 11 onto a single master curve, as the inset demonstrates. Note that for finite L the fronts of all systems eventually fix to one species. The fronts then show classical Eden roughening without any selective roughening. Any contribution of selective roughening to the overall width w decays and the width saturates according to the classical law, $w_{\text{sat}} \sim t^{1/2}$ [65].

To conclude, surface roughening close to criticality occurs in two regimes. Until crossover time $\tau_\times$, one observes Eden roughening, whereas for times larger than $\tau_\times$ selective roughening occurs until the front fixes to one species. The dynamics of the width of the front is summarized by

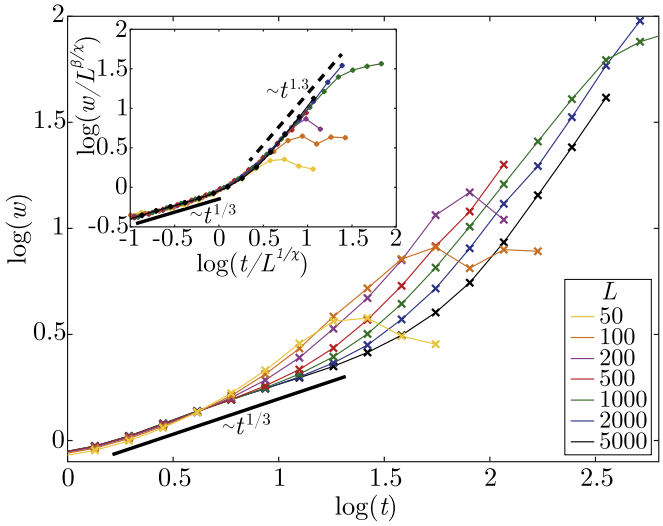

Figure 11. The width w of the front plotted versus time for several system sizes L close to the critical point at $\mathcal{T} = \mathcal{T}_c \approx 1.6$. Inset: after rescaling time t by $\tau_\times \sim L^{1/\chi}$ and width w by $w_\times \sim L^{\gamma/\chi}$, the curves collapse onto a single master curve. The solid black line indicates Eden roughening with $w \sim t^{1/3}$, whereas the dashed black line shows selective roughening with $w \sim t^{1.3}$ for $t \gg \tau_\times$. Note that the saturation of w at large times is due to the finite system size and the fact that we only sample from realizations where the front has not yet fixed to a single species (see main text for details).

$$w(L, t) \sim \begin{cases} t^{\gamma} & t \ll \tau_\times \sim L^{1/\chi}, \\ t^{\gamma'} L^{(\gamma-\gamma')/\chi} & t \gg \tau_\times. \end{cases} \tag{12}$$

5. Summary and conclusion

In this work we studied a generalized Eden model, where two species compete with each other at the rough expanding front. Individuals of the two species influence each other by frequency-dependent selection, which acts between nearest neighbors. We analyzed the evolutionary dynamics at the expanding front, where single-species sectors form and coarsen. Ultimately, the front fixes to one species, which we identify with an absorbing state of our model.

In its general form the model can implement several scenarios including selective advantage, and also well-known game theoretical settings like the snow drift game or the coordination game. Each of them creates distinct patterns, which should be analyzed in detail in future work. For the prominent example of a public goods game, we find that cooperators prevail in a wide parameter regime, as expected for a spatial version of a social dilemma [15, 45–47]. For other parameter values defectors take over the front, as usual.

We identify the transition between long-term cooperation and long-term defection as a nonequilibrium critical phase transition between two absorbing states. The set of critical exponents (see table 1), which we determined by analyzing critical and finite size scaling, shows that the phase transition belongs to a new universality class. We attribute this result to the fact that the front in our model is rough and not flat as in usual absorbing states. Close to the critical transition the front's roughness exhibits a crossover in time from slow Eden roughening to fast selective roughening. Strong roughening has also been observed at phase transitions in a related model by Lavrentovich and Nelson [81].

Our present work does not include creation of boundaries by mutations or other means. Therefore, sectors are compact, a property shared with regular CDP with a flat front [78]. Note however, that we found exponents different from that of the flat CDP universality class, see table 1. This is not astonishing, since not only do we treat rough fronts, but there also exists no symmetry when we exchange defectors and cooperators (besides at $\mathcal{R} = \mathcal{T} = 0$), whereas there is an exact symmetry upon exchange of active and inactive sites in CDP.

For continuous phase transitions the critical exponents and the transverse dimension d of the system are usually related to each other by hyperscaling relations [74, 75], at least below an upper critical dimension d_c. For systems with several absorbing states a so-called generalized hyperscaling relation exists [82]

$$d\nu_\perp = \nu_\parallel \Theta + \beta + \beta'. \tag{13}$$

This relation 'holds for almost all universality classes of absorbing phase transitions below their upper critical dimension' as Henkel *et al* state in [75], however, without giving any counterexample. The critical exponents

determined in our present work (see table 1) violate the above equation for $d = 1$. It might therefore be that our model has a critical dimension d_c smaller than 1. An alternative explanation may be that the enhanced roughness of the front leads to an effective dimension larger than one similar to models of surface growth, which create fronts with fractal properties [65]. Interestingly, in an earlier work [69] we also found enhanced roughness in the expanding front at the phase transition. There, the generalized hyperscaling relation was fulfilled within the margin of error of the critical exponents.

The roughness of the front correlates with superdiffusive motion of the boundaries separating sectors. Two factors contribute to the movement of the boundaries on long length scales. On the one hand, the direct competition between the species on either side of the boundaries pushes them towards the sector composed of the more slowly reproducing species. On the other hand, boundaries follow the local tilt of the front. In the public goods game cooperator sectors are advanced, while defector sectors lag behind. Near the critical transition, defectors outcompete their direct cooperating neighbors but the front is tilted towards sectors filled by defectors, so the two factors move the boundaries in opposite directions. At the phase transition both effects cancel and the front fixes with equal probability to either species. The strong roughening correlates with superdiffusive motion of the boundaries with nearly ballistic scaling.

Accordingly, whether a species takes over the expanding front is determined by two contributions: its reproduction rate relative to its competitor and its position relative to the average front position. The influence of different reproduction rates of neighboring species can directly be compared and is summarized in the phrase 'survival of the fittest'. The position at the front determines the available space for progeny, which then have the opportunity to expand sidewards. This is illustrated by the phrase 'survival of the fastest' [39].

In our model the number of sectors only decreases. It does not include experiments with mutually beneficial interactions between different species, which do not generate sectors [38, 83, 84]. In future extensions of our model this may be remedied by including motility of individuals [85, 86], by allowing reproduction to more distant lattice sites [81], or by increasing the maximal number of individuals per lattice site from one. Moreover, it is worthwhile to consider interactions ranging beyond nearest neighbors, since biomolecules, released by individual microorganisms, may diffuse in the extracellular medium [87–89]. In the public goods game scenario this would stabilize narrow sectors of defectors so that they do not lose contact to the front.

In general, range expansion of multiple species will develop enhanced roughness at the growing front. As we demonstrated here, the corresponding models have new and interesting statistical properties. From a biological point of view, roughness is important. It affects the territories that different species occupy and thereby their evolutionary success through the strong random motion of sector boundaries. This may also be relevant for range expansion in a real environment and not just in a test tube. To better understand the properties and consequences of rough expanding fronts, further theoretical work is needed. At the same time further experiments should look for the fingerprint of roughness in microbial colony growth.

Acknowledgments

We thank the research training group GRK 1558 funded by Deutsche Forschungsgemeinschaft for financial support. We further thank Erwin Frey, Maria Eckl, Florian Gartner, and Raphaela Geßele for discussion and collaboration on a related model.

References

[1] Murray J D 2007 *Mathematical Biology :I. An Introduction* vol 1 3rd edn (Berlin: Springer)
[2] Griffiths R W, Schloesser D W, Leach J H and Kovalak W P 1991 Distribution and dispersal of the zebra mussel (*Dreissena polymorpha*) in the Great Lakes Region *Can. J. Fish. Aquat. Sci.* **48** 1381–8
[3] Loarie S R, Duffy P B, Hamilton H, Asner G P, Field C B and Ackerly D D 2009 The velocity of climate change *Nature* **462** 1052–5
[4] Chen I C, Hill J K, Ohlemuller R, Roy D B and Thomas C D 2011 Rapid range shifts of species associated with high levels of climate warming *Science* **333** 1024–6
[5] Peacock E *et al* 2015 Implications of the circumpolar genetic structure of polar bears for their conservation in a rapidly warming arctic *PLoS One* **10** e112021
[6] Stringer C 2003 Human evolution: out of ethiopia *Nature* **423** 692–5
[7] Liu H, Prugnolle F, Manica A and Balloux F 2006 A geographically explicit genetic model of worldwide human-settlement history *Am. J. Hum. Genet.* **79** 230–7
[8] Moreau C, Bherer C, Vezina H, Jomphe M, Labuda D and Excoffier L 2011 Deep human genealogies reveal a selective advantage to be on an expanding wave front *Science* **334** 1148–50
[9] Brú A, Albertos S, Luis Subiza J, García-Asenjo J L and Brú I 2003 The universal dynamics of tumor growth *Biophys. J.* **85** 2948–61
[10] Xavier J B 2011 Social interaction in synthetic and natural microbial communities *Mol. Syst. Biol.* **7** 483
[11] Hall-Stoodley L, Costerton J W and Stoodley P 2004 Bacterial biofilms: from the natural environment to infectious diseases *Nat. Rev. Micro.* **2** 95–108
[12] Nadell C D, Xavier J B and Foster K R 2009 The sociobiology of biofilms *FEMS Microbiol. Rev.* **33** 206–24
[13] Mitri S, Xavier J B and Foster K R 2011 Social evolution in multispecies biofilms *Proc. Natl Acad. Sci. USA* **108** (Suppl 2)10839–46

[14] Hofbauer J and Sigmund K 1998 *Evolutionary Games and Population Dynamics* 1st edn (Cambridge: Cambridge University Press)
[15] Szabó G and Fáth G 2007 Evolutionary games on graphs *Phys. Rep.* **446** 97–216
[16] Frey E 2009 Evolutionary game theory: theoretical concepts and applications to microbial communities *Physica* A **389** 4265–98
[17] Buckling A, Maclean R C, Brockhurst M A and Colegrave N 2009 The Beagle in a bottle *Nature* **457** 824–9
[18] Shapiro J A 1995 The significances of bacterial colony patterns *BioEssays* **17** 597–607
[19] Ben Jacob E, Aharonov Y and Shapira Y 1999 Bacteria harnessing complexity *Biofilms* **1** 239–63
[20] Golding I, Cohen I and Ben-Jacob E 1999 Studies of sector formation in expanding bacterial colonies *Europhys. Lett.* **48** 587–93
[21] Matsushita M, Wakita J, Itoh H, Watanabe K, Arai T, Matsuyama T, Sakaguchi H and Mimura M 1999 Formation of colony patterns by a bacterial cell population *Physica* A **274** 190–9
[22] Matsuyama T and Matsushita M 2001 Population morphogenesis by cooperative bacteria *Forma* **16** 307–26
[23] Nguyen B, Upadhyaya A, van Oudenaarden A and Brenner M P 2004 Elastic instability in growing yeast colonies *Biophys. J.* **86** 2740–7
[24] Vicsek T, Cserzo M and Horvath V K 1990 Self-affine growth of bacterial colonies *Physica* A **167** 315–21
[25] Wakita J-I, Itoh H, Matsuyama T and Matsushita M 1997 Self-affinity for the growing interface of bacterial colonies *J. Phys. Soc. Japan.* **66** 67–72
[26] Huergo M, Pasquale M, Bolzán A, Arvia A and González P 2010 Morphology and dynamic scaling analysis of cell colonies with linear growth fronts *Phys. Rev.* E **82** 031903
[27] Hallatschek O, Hersen P, Ramanathan S and Nelson D R 2007 Genetic drift at expanding frontiers promotes gene segregation *Proc. Natl Acad. Sci. USA* **104** 19926–30
[28] Derrida B and Dickman R 1991 On the interface between two growing Eden clusters *J. Phys. A: Math. Gen.* **24** L191–5
[29] Saito Y and Müller-Krumbhaar H 1995 Critical phenomena in morphology transitions of growth models with competition *Phys. Rev. Lett.* **74** 4325–8
[30] Crespi B J 2001 The evolution of social behavior in microorganisms *Trends Ecol. Evol.* **16** 178–83
[31] Velicer G J 2002 Social strife in the microbial world *Trends Microbiol.* **11** 330–7
[32] Griffin A S, West S A and Buckling A 2004 Cooperation and competition in pathogenic bacteria *Nature* **430** 1024–7
[33] Kreft J U 2004 Conflicts of interest in biofilms *Biofilms* **1** 265–76
[34] West S A, Diggle S P, Buckling A, Gardner A and Griffin A S 2007 The social lives of microbes *Annu. Rev. Ecol. Evol. Syst.* **38** 53–77
[35] Hibbing M E, Fuqua C, Parsek M R and Peterson S B 2010 Bacterial competition: surviving and thriving in the microbial jungle *Nat. Rev. Micro.* **8** 15–25
[36] Mitri S and Richard Foster K 2013 The genotypic view of social interactions in microbial communities *Annu. Rev. Genet.* **47** 247–73
[37] Gore J, Youk H and van Oudenaarden A 2009 Snowdrift game dynamics and facultative cheating in yeast *Nature* **459** 253–6
[38] Müller M JI, Neugeboren B I, Nelson D R and Murray A W 2014 Genetic drift opposes mutualism during spatial population expansion *Proc. Natl Acad. Sci. USA* **111** 1037–42
[39] van Dyken J D, Müller M JI, Mack K ML and Desai M M 2013 Spatial population expansion promotes the evolution of cooperation in an experimental Prisoner's Dilemma *Curr. Biol.* **23** 919–23
[40] Darwin C 1859 *On the Origin of Species by Means of Natural Selection, or the Preservation of Favoured Races in the Struggle for Life* (London: John Murray)
[41] Axelrod R 2009 *The Evolution of Cooperation* revised edition (New York: Basic Books)
[42] Korolev K S 2013 The fate of cooperation during range expansions *PLoS Comput. Biol.* **9** e1002994
[43] Rainey P B and Rainey K 2003 Evolution of cooperation and conflict in experimental bacterial populations *Nature* **425** 72–74
[44] Chuang J S, Rivoire O and Leibler S 2009 Simpson's paradox in a synthetic microbial system *Science* **323** 272–5
[45] Nowak M A, Bonhoeffer S and May R M 1994 Spatial games and the maintenance of cooperation *Proc. Natl Acad. Sci. USA* **91** 4877–81
[46] Ohtsuki H, Hauert C, Lieberman E and Nowak M A 2006 A simple rule for the evolution of cooperation on graphs and social networks *Nature* **441** 502–5
[47] Fu F, Nowak M A and Hauert C 2010 Invasion and expansion of cooperators in lattice populations: Prisoner's dilemma vs. snowdrift games *J. Theor. Biol.* **266** 358–66
[48] Melbinger A, Cremer J and Frey E 2010 Evolutionary game theory in growing populations *Phys. Rev. Lett.* **105** 178101
[49] Cremer J, Melbinger A and Frey E 2012 Growth dynamics and the evolution of cooperation in microbial populations *Sci. Rep.* **2** 281
[50] Xavier J B and Foster K R 2007 Cooperation and conflict in microbial biofilms *Proc. Natl Acad. Sci. USA* **104** 876–81
[51] Nadell C D, Foster K R and Xavier J B 2010 Emergence of spatial structure in cell groups and the evolution of cooperation *PLoS Comput. Biol.* **6** e1000716
[52] Greig D and Travisano M 2004 The Prisoner's Dilemma and polymorphism in yeast SUC genes *Proc. Biol. Sci* **271** S25–6
[53] Koschwanez J H, Foster K R and Murray A W I 2011 *PLoS Biol.* **9** e1001122
[54] sen Datta M, Korolev K S, Cvijovic I, Dudley C and Gore J 2013 Range expansion promotes cooperation in an experimental microbial metapopulation *Proc. Natl. Acad. Sci. USA* **110** 7354–9
[55] Pattus F and Abdallah M A 2000 Siderophores and iron-transport in microorganisms *J. Chin. Chem. Soc.* **47** 1–20
[56] Ratledge C and Dover L G 2000 Iron metabolism in pathogenic bacteria *Annu. Rev. Microbiol.* **54** 881–941
[57] Nadell C D and Bassler B L 2011 A fitness trade-off between local competition and dispersal in *Vibrio cholerae* biofilms *Proc. Natl Acad. Sci. USA* **108** 14181–5
[58] van Gestel J, Weissing F J, Kuipers O P and Kovács A T 2014 Density of founder cells affects spatial pattern formation and cooperation in Bacillus subtilis biofilms *ISME J.* **8** 2069–79
[59] Riley M A and Gordon D M 1999 The ecological role of bacteriocins in bacterial competition *Trends Microbiol.* **7** 129–33
[60] Cornforth D M and Foster K R 2013 Competition sensing: the social side of bacterial stress responses *Nat. Rev. Micro.* **11** 285–93
[61] Lee V T and Schneewind O 2001 Protein secretion and the pathogenesis of bacterial infections *Genes Dev.* **15** 1725–52
[62] Weber M F, Poxleitner G, Hebisch E, Frey E and Opitz M 2014 Chemical warfare and survival strategies in bacterial range expansions *J. R. Soc. Interface* **11** 20140172
[63] Xavier J B, Kim W and Foster K R 2011 A molecular mechanism that stabilizes cooperative secretions in *Pseudomonas aeruginosa Mol. Microbiol.* **79** 166–79
[64] Eden M 1960 A two-dimensional growth process *Proc. 4th Berkeley Symp. on Mathematical Statistics and Probability* vol 4 pp 223–39
[65] Barabási A-L and Stanley H E 1995 *Fractal concepts in surface growth* 1st edn (Cambridge: Cambridge University Press)
[66] Plischke M and Rácz Z 1985 Dynamic scaling and the surface structure of Eden clusters *Phys. Rev.* A **32** 3825–8
[67] Jullien R and Botet R 1985 Scaling properties of the surface of the Eden model in $D = 2, 3, 4$ *J. Phys. A: Math. Gen.* **18** 2279–87
[68] Ali A and Grosskinsky S 2010 Pattern formation through genetic drift at expanding population fronts *Adv. Complex Syst.* **13** 349–66

[69] Kuhr J-T, Leisner M and Frey E 2011 Range expansion with mutation and selection: dynamical phase transition in a two-species Eden model *New J. Phys.* **13** 113013
[70] Gillespie D T 1976 A general method for numerically simulating the stochastic time evolution of coupled chemical reactions *J. Comput. Phys.* **22** 403–34
[71] Jullien R and Botet R 1985 Surface thickness in the Eden model *Phys. Rev. Lett.* **54** 2055
[72] Krug J and Spohn H 1992 Kinetic roughening of growing surfaces *Solids far from Equilibrium* ed C Godrèche (Cambridge: Cambridge University Press)
[73] Halpin-Healy T and Zhang Y-C 1995 Kinetic roughening phenomena, stochastic growth, directed polymers and all that, aspects of multidisciplinary statistical mechanics *Phys. Rep.* **254** 215–414
[74] Ódor G 2004 Universality classes in nonequilibrium lattice systems *Rev. Mod. Phys.* **76** 663–724
[75] Henkel M, Hinrichsen H and Lübeck S 2008 *Non-equilibrium Phase Transitions: Absorbing Phase Transitions* vol 1 1st edn (Berlin: Springer)
[76] Hamilton W D 1964 The genetical evolution of social behaviour. I *J. Theor. Biol.* **7** 1–16
[77] Hamilton W D 1964 The genetical evolution of social behaviour. II *J. Theor. Biol.* **7** 17–52
[78] Essam J W 1989 Directed compact percolation: cluster size and hyperscaling *J. Phys. A: Math. Gen.* **22** 4927
[79] Lübeck S 2006 Crossover scaling in the Domany-Kinzel cellular automaton *J. Stat. Mech. Theor. Exp.* **2006** P09009
[80] Kardar M, Parisi G and Zhang Y-C 1986 Dynamic scaling of growing interfaces *Phys. Rev. Lett.* **56** 889–92
[81] Lavrentovich M O and Nelson D R 2014 Asymmetric mutualism in two- and three-dimensional range expansions *Phys. Rev. Lett.* **112** 138102
[82] Mendes J F F, Dickman R, Henkel M and Marques M C 1994 Generalized scaling for modes with multiple absorbing states *J. Phys. A: Math. Gen.* **27** 3019–28
[83] Momeni B, Brileya K A, Fields M W and Shou W 2013 Strong inter-population cooperation leads to partner intermixing in microbial communities *eLife* **2** e00230
[84] Kovács A T 2014 Impact of spatial distribution on the development of mutualism in microbes *Front. Microbiol.* **5** 649
[85] Reichenbach T, Mobilia M and Frey E 2007 Mobility promotes and jeopardizes biodiversity in rock-paper-scissors games *Nature* **448** 1046–9
[86] Gelimson A, Cremer J and Frey E 2013 Mobility, fitness collection, and the breakdown of cooperation *Phys. Rev.* E **87** 042711
[87] Julou T, Mora T, Guillon L, Croquette V, Schalk I J, Bensimon D and Desprat N 2013 Cell–cell contacts confine public goods diffusion inside *Pseudomonas aeruginosa* clonal microcolonies *Proc. Natl Acad. Sci. USA* **110** 12577–82
[88] Allen B, Gore J, Nowak M A and Bergstrom C T 2013 Spatial dilemmas of diffusible public goods *eLife* **2** e01169
[89] Menon R and Korolev K S 2015 Public good diffusion limits microbial mutualism *Phys. Rev. Lett.* **114** 168102